MIT Libraries | DSpace@MIT

MIT Open Access Articles

Two-cycle pulse generation from mode-locked Kerr frequency combs based on an integrated dispersion-flattened micro-resonator

Massachusetts Institute of Technology

Two-cycle pulse generation from mode-locked Kerr frequency combs based on an integrated dispersion-flattened micro-resonator

Lin Zhang, Anuradha M. Agarwal, Lionel C. Kimerling, and Jurgen Michel

Microphotonics Center and Department of Materials Science and Engineering, Massachusetts Institute of Technology, Cambridge, MA 02139, USA

Email: linzhang@mit.edu

ABSTRACT

Kerr frequency comb generation from a nonlinear high-Q resonator becomes an interdisciplinary research topic emerging from nonlinear optics, integrated photonics, and ultrafast optics. We show that ultrashort cavity solitons can be generated from a mode-locked Kerr frequency comb in a dispersion-engineered nonlinear microresonator. The spectral flatness of the comb is greatly improved by making the cavity soliton as short as two optical cycles, with a comb line power variation below 20 dB over an octave-spanning bandwidth from near infrared to mid infrared, while excellent spectral coherence is achieved by soliton-based mode locking. It is shown by simulation that the two-cycle solitons are robust to the wideband soliton perturbation effects such as all-order dispersion, frequency-dependent Q-factor, dispersive wave generation, Kerr self-steepening, and stimulated Raman scattering. The pump power used to generate an octave-spanning combs can be significantly reduced when a dispersion profile with four zero-dispersion frequencies, which paves the way to achieve a fully integrated frequency comb generator on a chip.

Keywords: Micro-resonator, microring, silicon photonics, frequency comb, dispersion engineering, mode-locking

I. Introduction

Implementation of broadband optical frequency combs [1, 2] based on ultrafast mode-locked lasers [3] has fueled revolutionary advances in numerous optics and photonics branches, such as precision metrology, spectroscopy and sensing, and signal processing [4-7]. In particular, octave-spanning frequency comb generation opens a great opportunity to achieve extremely accurate timing and positioning, explore ultrafast electronic and photonic dynamics of the microscopic world, and provide ultra-broadband information acquisition and processing capability for a wide range of civil and military applications [8].

Resonance-enhanced optical nonlinearity in high-Q-factor micro-resonators [9] facilitates nonlinear spectral broadening of incoming light waves to effectively generate broadband optical frequency combs [10-17]. This type of frequency comb generation is enabled by Kerr nonlinearities, such as cascaded four-wave mixing and modulational instability, sometimes called Kerr frequency combs. The micro-resonator-based comb generators with a high Q-factor exhibit a great potential to achieve compact, light-weight, power-efficient and cost-effective (sub) systems for information acquisition and processing with high signal integrity [8]. Various types of micro-resonators based on different material platforms have been demonstrated as an efficient frequency comb generator [10-17]. Mode-locking of Kerr frequency combs has been shown to be possible [18-20] with excellent spectral coherence [19], which is associated with cavity soliton formation [21]. On the other hand, octave-spanning Kerr combs have been shown experimentally [22, 23]. It would be desirable to improve the bandwidth of mode-locked Kerr frequency combs and increase comb line power especially at the wings of comb spectra, which is important in frequency metrology and sensing applications.

In the soliton-based mode-locking case, the comb line power always decreases (except at the location of dispersive waves). To achieve excellent spectral coherence and flatness simultaneously in Kerr comb generation, one needs to produce narrower cavity solitons whose spectral width represents the comb bandwidth. In theory, when higher-order dispersion and nonlinear soliton perturbation effects e.g., Kerr self-steepening are ignored, the soliton pulsewidth or the mode-locked Kerr comb's bandwidth is directly related to the nonlinear coefficient of the cavity, pump power, resonance finesse, and the second-order chromatic dispersion [19, 24]. We note that the nonlinear coefficient is primarily

determined by the material that is used to form a resonator, while the finesse is highly dependent on cavity loss and accordingly the fabrication process. One way to increase the comb bandwidth is to reduce the dispersion coefficient [19, 24]. For a wideband comb, it is highly desirable to have all frequency components contained in a soliton spectrum see the low dispersion. In this sense, the dispersion needs to be low and wavelength insensitive in the anomalous dispersion regime, which is the goal of dispersion engineering in this work.

Fortunately, chromatic dispersion in integrated waveguides and cavities is highly tailorable [25-30]. In strip or rib waveguides, one has a relatively small parameter set to use for dispersion engineering, and there is a general trade-off between anomalous dispersion bandwidth and dispersion peak value. That is, when the anomalous dispersion is tailored to be small to produce a short cavity soliton, the dispersion bandwidth also decreases and cannot accommodate a wide comb (soliton) spectrum. Using a nano-slot waveguide, one can flatten the dispersion profile [28, 29], maintaining a small anomalous dispersion while extending the dispersion bandwidth. This dispersion tailoring technique has been shown to be useful in on-chip supercontinuum generation [31]. More importantly, this technique is applicable to different wavelength ranges from near infrared to mid infrared [32] and various material platforms [31, 33, 34].

In this paper, we explore the use of dispersion-flattened nonlinear microring resonators for mode-locked octave-spanning Kerr comb generation, with greatly improved comb flatness as a result of two-cycle cavity soliton formation. The influence of soliton perturbation effects on the required pump power is discussed. Intriguingly, we show that a flat and low dispersion with four zero-dispersion wavelengths (i.e., the low-dispersion band contains both normal and anomalous dispersions) could be more favorable to reduce the required pump power. Identified as a unique feature for cavity soliton, this verifies the robustness of two-cycle cavity soliton formation.
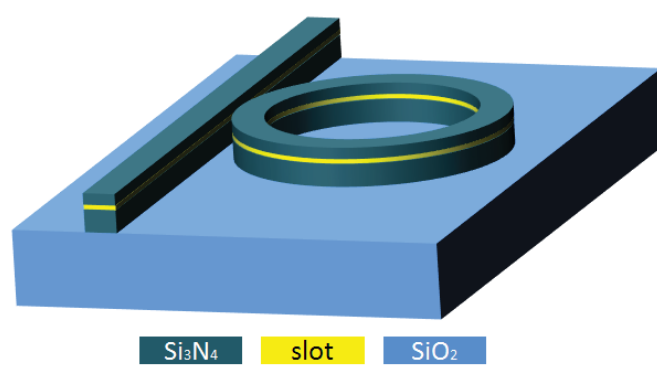

Fig. 1. A microring resonator based on dispersion-flattened silicon nitride slot waveguides for Kerr frequency comb generation. The horizontal slot is made of silica in this case.

II. Frequency Dependence of Cavity Parameters

To show the role of flattened dispersion in improving the Kerr frequency comb performance, we start with a specific cavity design. As shown in Fig. 1, the waveguide has a 156-nm low-index silica slot between two high-index Si_3N_4 layers that are 920-nm and 480-nm thick, respectively. The waveguide width is 1300 nm. A microring resonator is formed with a bending radius of about 114 µm to obtain a free spectral range (FSR) of 200 GHz. The cavity is coupled to a straight waveguide in the same structure with a gap of 450 nm. The substrate is 3-µm-thick buried oxide (BOX), and the upper cladding is air.

Since we look at octave-spanning frequency comb generation, it becomes critically important to examine the dependence of every cavity parameter on frequency over such a wide bandwidth. Chromatic dispersion has been carefully flattened using the dispersion engineering technique assisted by a nano-slot [28, 29]. As shown in Fig. 2(a), a flat and low dispersion is obtained in the anomalous dispersion regime. Two ZDWs are located at 1140 and 2304 nm, separated by one octave. The 2nd-order dispersion coefficient β_2 varies from 0 to 0.016 ps^2/m, and accordingly the dispersion value D changes within 0~17 ps/(nm·km). Note that $\beta_2 = -\lambda^2 D/2\pi c$, where λ is the

wavelength and c is the speed of light in vacuum. In this work, we tailor the dispersion profile D(λ) to produce a relatively flat $β_2$. Another important cavity parameter is the nonlinear coefficient, γ. Over the spectral band of interest, where the dispersion has been flattened, we calculate the nonlinear coefficient as a function of frequency using a full-vector formula [35]. Simulations show that the wavelength-dependent nonlinear coefficient varies by almost one order of magnitude. This is associated with the Kerr self-steepening effect and produces higher nonlinear gain at high frequencies.

Aiming at an octave-spanning bandwidth, we also note that both, round-trip loss α and coupling coefficient κ, strongly depend on wavelength. Confinement loss (i.e., power leakage to the silicon substrate below BOX) is computed as a function of wavelength using a full-vector mode solver (COMSOL). From literature [14, 17, 36], a scattering loss below 0.2 dB/cm is possible, and we use this value for 1.55 µm wavelength, where the confinement loss is less than 0.0001 dB/cm. In theory, scattering loss is dependent on frequency [37], so we scale the loss of 0.2 dB/cm and obtain the wavelength dependent scattering loss. Figure 2(b) shows the spectral change of α, with both confinement loss and scattering loss included. The coupling coefficient κ is obtained as a function of wavelength from 3D electro-magnetic wave simulations. The 450-nm gap between the closest sidewalls of the ring and the waveguide is set to achieve critical coupling near 1.55 µm. As shown in Fig. 2(c), κ changes with wavelength more quickly than round-trip loss and becomes as high as 0.6 at 2.8 µm, although κ is only 0.0038 at 1.55 µm. This causes strong spectral dependence of the cavity Q-factor. The Q-factor varies by almost three orders of magnitude in the bandwidth of interest. At 1.55 µm, cavity Q-factor is $2.7×10^5$, and the associated finesse is 281. The nonlinear coefficient γ is 0.9 /(W·m).

(a)   (b)
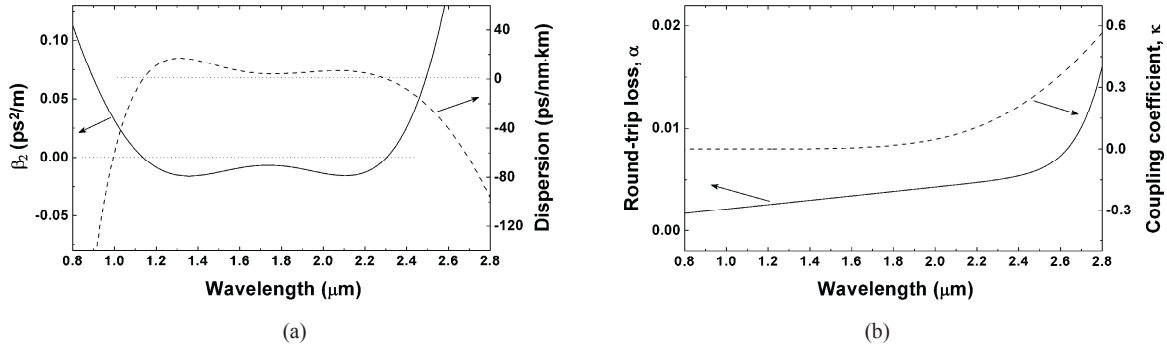
Fig. 2. Frequency dependence of cavity parameters, including (a) second-order dispersion, and (b) cavity loss and coupling between the ring resonator and waveguide.

III. Numerical Model

To simulate the Kerr frequency comb generation, we use the driven and damped nonlinear Schrödinger equation [18, 38] (also called Lugiato-Lefever equation [39-41]) as follows:

$$t_R \frac{\partial E}{\partial t} = \sqrt{\kappa_0} E_{in} + l[K(E) + R(E)] - \left(\frac{\alpha}{2} + \frac{\kappa}{2} - j\delta_0 + jl \sum_{m=2}^{\infty} \frac{(-j)^m \beta_m}{m!} \frac{\partial^m}{\partial \tau^m} \right) E$$

where $E=E(τ,t)$ and E_{in} are intra-cavity field and input field (pump power $P_{in} = |E_{in}|^2$), τ and t are the fast and slow times, and $κ_0$ is the coupling coefficient at the pump location. t_R is the round-trip time, and $δ_0$ is the cavity phase detuning defined as $δ_0 = τ_0·(ω_n - ω_0)$, where $ω_0$ and $ω_n$ are the pump's angular frequency and the nth angular resonance frequency near the pump. Other linear cavity parameters include the power loss per round trip α, the power coupling coefficient κ, and the mth dispersion coefficient $β_m$. Since a flat and low dispersion has a small $β_2$ over a wide bandwidth, it is important to take the higher-order dispersion into account. The all-order dispersion (AOD) terms can be treated in frequency domain as in [40].

Similarly, the spectral dependence of α and κ is included in frequency domain as well, which can be treated as part of the dispersion term. Kerr and Raman nonlinearities are taken into account in the following way:

$$K(E) = -i\gamma_K(1 - i\tau_{shock\_K}\frac{\partial}{\partial t})E|E|^2$$

$$R(E) = -i\gamma_R(1 - i\tau_{shock\_R}\frac{\partial}{\partial t})[E\int_{-\infty}^{t} h_R(t - t')|E|^2 dt']$$

where the Kerr nonlinear coefficient γ_K, the Raman gain coefficient γ_R, and the Raman response function h_R are defined the same way as in [42]. The Kerr and Raman shock times τ_{shock_K} and τ_{shock_R} represent the derivatives of γ_K, and γ_R, with respect to frequency [43]. In our simulations, the temporal step is 1 fs, and the round-trip time is 5 ps (FSR is 200 GHz).
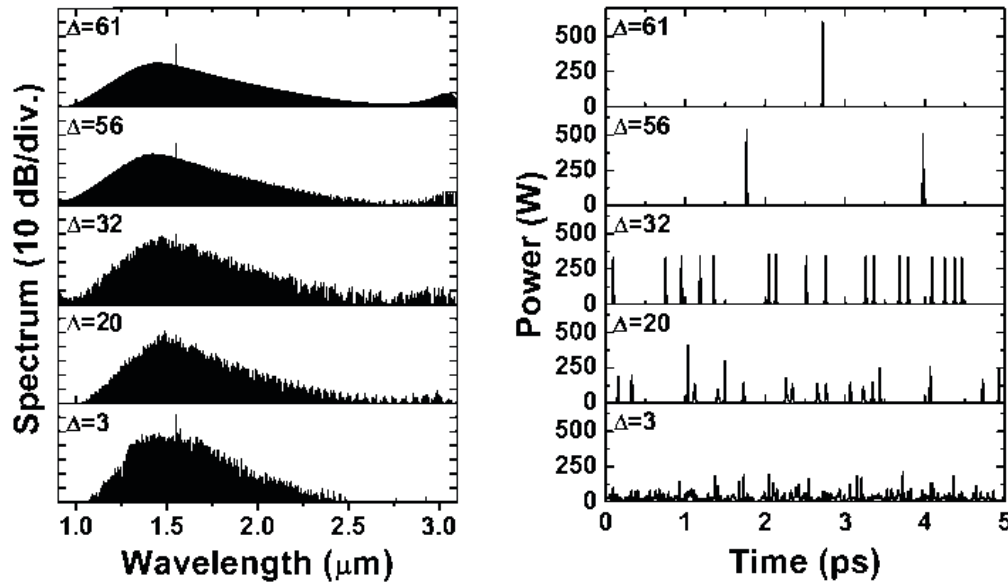

Fig. 3. Comb spectrum evolution at different pump detunings. The comb lines become increasingly coherent to each other, with a single cavity soliton eventually formed per round trip.

IV. Two-cycle Cavity Soliton Generation from Kerr Frequency Combs

We pump the cavity at the resonance adjacent to 1.55 μm, which is almost at the center of the small anomalous dispersion band, with a continuous wave (CW) laser power of 1.6 W. We slightly detune the pump every 20 ns to be closer to the resonance from the short wavelength side. Here, we temporarily ignore the Kerr self-steepening effect and stimulated Raman scattering terms. The intra-cavity comb spectrum evolution can be found in Fig. 3, shown by spectral and temporal snapshots at a normalized detuning Δ=3, 20, 32, 56, and 61 (Δ is defined as $2\delta_0/(\alpha+\kappa)$ [24], representing detuning measured in terms of resonance linewidth). The comb spectrum becomes increasingly smooth, and accordingly the intra-cavity field evolves into a pulsed waveform. The reason behind this behavior is that the pump detuning triggers a transition of the generated comb from the modulation instability regime to the cavity soliton regime, and a similar process has been identified and described in [19, 24, 44]. Red-shifting the pump and making it further tuned into resonance reduces the number of cavity solitons over one round trip time, as can be seen in Fig. 3 with the detuning Δ increased from 32 to 61. Finally, a single soliton is formed with a full-width at half maximum (FWHM) of 7.67 fs and a peak power of 602 W. The pulse width is corresponding to 1.5 optical cycles at 1.55 μm wavelength. The generated comb at Δ=61 has an improved spectral flatness of comb lines, with a 20-dB comb-line power change over an octave-spanning bandwidth from 1.11 to 2.22 μm. One can see a weak dispersive wave at ~3 μm, due to a degraded cavity Q-factor at long wavelengths.
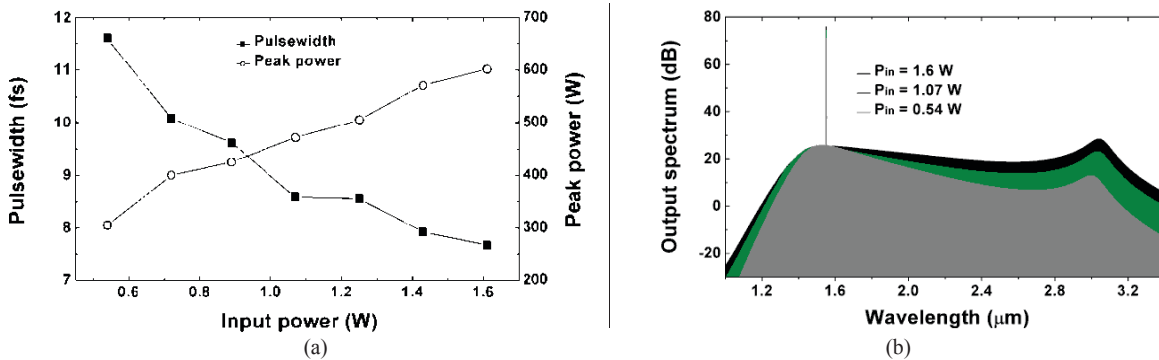
Fig. 4. (a) Cavity soliton's pulsewidth increases from 7.67 fs (1.5 optical cycles) to 11.6 fs (2.2 optical cycles) as the pump power is reduced, and the peak power decreases to 305 W. (b) Output comb spectra at the output port of the waveguide for a pump power of 1.6, 1.07, and 0.54 W, respectively. Comb line power can be efficiently coupled out from the cavity at long wavelengths.

It is important to note that, in the simulation above, the pump power of 1.6 W is in the waveguide. This means much higher power is required off-chip before coupling to the device chip, considering a typical coupling loss of 5~10 dB. It would be of great interest to examine the comb performance with a low pump power. Figure 4(a) shows that the pulsewidth increases from 7.67 to 11.6 fs (2.2 optical cycles) as the pump power is reduced from 1.6 to 0.54 W. Accordingly, the soliton peak power decreases to 305 W. On the other hand, further increasing the pump power, we find the pulse width saturated at around 7.5 fs.

The comb spectrum at the waveguide output port is shown in Fig. 4(b) for an input pump power P_{in} = 1.6, 1.07, and 0.54 W. Since the coupling coefficient between the cavity and the waveguide greatly increases with wavelength, the output comb spectrum has high comb line power at long wavelengths. Without the silica absorption added, the small spectral power change is 9.5, 11, and 19 dB, respectively, over an octave-spanning bandwidth from 1.5 to 3 µm. The excellent spectral flatness emphasizes the importance of removing O-H bond in silica. If the silica absorption is measured under some fabrication conditions and included into the model, spectral power is expected to drop beyond 2.6 µm. Using the band from 1.25 to 2.5 µm for octave-spanning applications to avoid the absorption in silica, we see that the comb line at 2.5 µm has a power lower than the highest comb line by 6.6, 11, and 18 dB for P_{in} = 1.6, 1.07, and 0.54 W, respectively.

V. Pump Power Reduction with Partially Normal Dispersion

The slot waveguide that is used to form the nonlinear microring resonator can produce a dispersion profile with four zero-dispersion wavelengths (ZDWs) when the upper silicon nitride height is slightly changed [29]. It would be interesting to explore the Kerr frequency comb generation with this type of "complicated" dispersion conditions. First, it is well-known that an optical soliton can be supported in the anomalous dispersion regime in a straight waveguide case [45]. Soliton will break if a normal dispersion region occurs in the middle of an anomalous dispersion band. However, in the cavity context, an external pump is used to maintain a stable cavity soliton, which might be more tolerant to the dispersion modification. This has not been explored before. Moreover, once the dispersion profile is moved toward to the normal dispersion regime, the overall dispersion becomes less, and other soliton perturbation effects will be more dominant. These include dispersive wave generation (DWG), frequency-dependent Q-factor (FDQ), Kerr self-steepening (KSS), and stimulated Raman scatter (SRS). It would be interesting to examine the influence of these effects. More importantly, in the engineering domain, we note that since the two-cycle cavity solitons have a very broad bandwidth, the dispersion experienced by the soliton is definitely not a dispersion at a specific frequency, and the soliton sees an average dispersion value. Therefore, if we produce a partially normal but average anomalous dispersion, we will be able to effectively reduce the average dispersion value. This would either result in a further increased comb bandwidth, or a reduced pump power requirement with comb bandwidth kept the same.
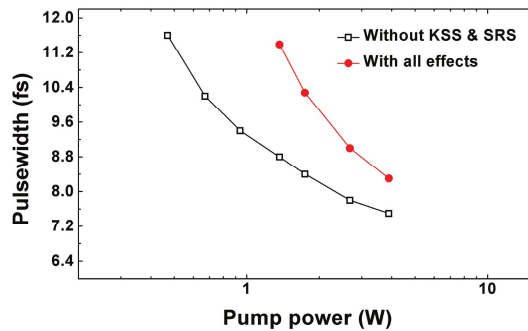
Fig. 5. Cavity soliton pulsewidth is examined as a function of pump power and is compared in two cases: with and without KSS and SRS effects. DWG and FDQ are included in the simulations in both cases.

We re-simulate the Kerr frequency comb generation with KSS and SRS included in the model, and all other parameters are the same. From Fig. 5, it is noted that two-cycle cavity solitons can still be generated with a pulsewidth of 10 fs. However, the required pump power is increased to around 2 W. This is a significant power requirement, considering that, with a coupling loss of 3~10 dB from an off-chip pump to an on-chip microresonator, a very high-power optical amplifier would be needed to provide such a CW pump. It is thus highly desirable to re-tailor the dispersion and mitigate the pump power problem.

By increasing the upper silicon nitride height from 480 to 500 nm, one can produce a set of dispersion profiles from the slot-assisted microring resonator, with increasingly more normal dispersion involved. As shown in Fig. 6, the dispersion is made to be partially normal but averagely anomalous, with another two ZDWs appearing in the middle. Four waveguides (WG1~WG4) are corresponding to an upper silicon nitride height of 480, 490, 495, and 500 nm
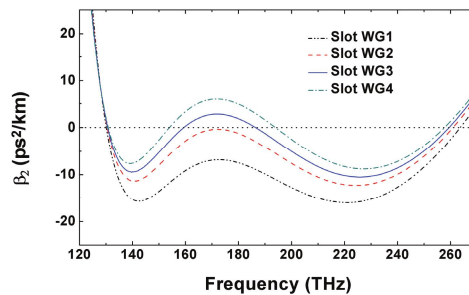

Fig. 6. Four waveguides (WGs) with re-tailored dispersion. WG1 has the dispersion shown in Fig. 2(a), and the other WGs have increasingly more normal dispersion appearing in the overall dispersion profile.

Pumping at 200 THz with a variable CW power, we first simulate the Kerr frequency comb generation with mode-locked comb lines in a case with all-order dispersion only and without KSS, FDQ, SRS, and DWG. In this way, we can examine whether or not such a dispersion profile with four ZDWs can support a cavity soliton in a relatively pure case. As shown in Fig. 7(a), it is found that the formation of a cavity soliton is possible for all four waveguides, and very short pulsewidth around 7 fs can be obtained. As expected, the required pump power is reduced in the case with partially normal but averagely anomalous dispersion. The more normal dispersion involved in the dispersion profile, the lower pump power is needed. However, it is important to mention that the cavity soliton will not be maintained if the pump is shifted to the frequency range with normal dispersion. By including the other four soliton perturbation effects in the simulations, we obtain larger soliton pulsewidth which is increased from 7 fs to 10 fs. Although significant reduction in the required pump power is also seen in Fig. 7(b), WG4 is not the case with the lowest pump power. In fact, the cavity soliton needs a little bit more anomalous dispersion to be tolerant to the other perturbations.
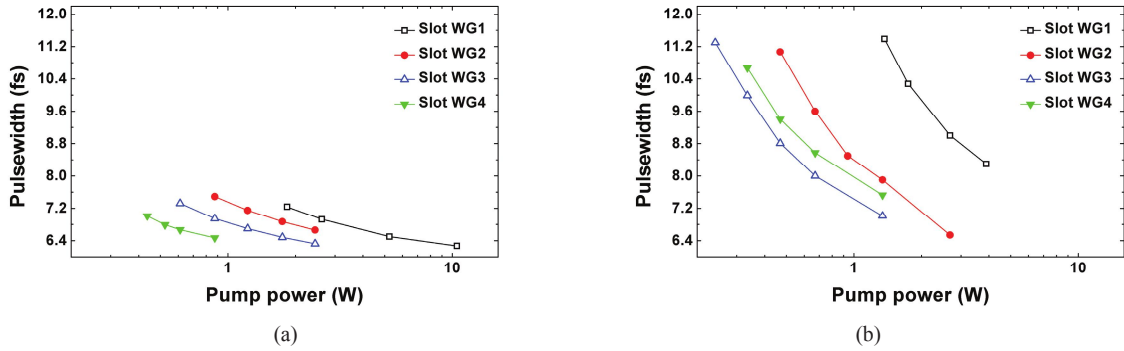
Fig. 7. (a) Cavity soliton pulsewidth is examined with different dispersion profiles in the case with only all-order dispersion and other perturbation effects removed from the model. (b) Soliton pulsewidth varies as a function of pump power with the same dispersion profiles but KSS, SRS, DWG, and FDQ are included in the simulations.
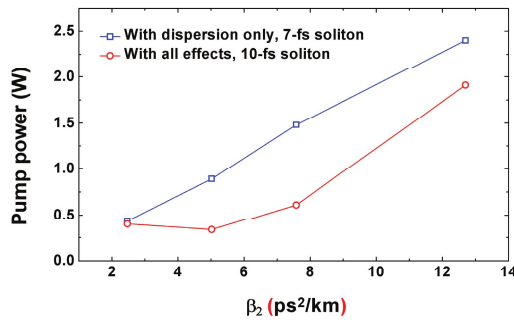

Fig. 8. Four waveguides (WGs) with re-tailored dispersion. WG1 has the dispersion shown in Fig. 2(a), and the other WGs have increasingly more normal dispersion appearing in the overall dispersion profile.

We examine the required pump power as a function of dispersion in both cases in Fig. 8. For all-order dispersion only, we keep the soliton pulsewidth at 7 fs. When all perturbation effects are included, we fix the pulsewidth at 10 fs. As shown in Fig. 8, the pump power almost linearly decreases with dispersion from 2.4 W to 437 mW in the case with dispersion only. In contrast, if the other soliton perturbations are considered, the pump power reduction can be saturated, which first decreases from 1.91 W to 335 mW and then increases to 400 mW.

VI. Summary and Outlook

In summary, we have shown that dispersion engineering in an integrated micro-resonator is critically important to increase the bandwidth of mode-locked Kerr frequency combs. The slot-assisted dispersion flattening technique has a great potential to enable the implementation of on-chip comb generators with excellent spectral coherence and flatness. Moreover, this dispersion engineering scheme provides us with a previously inaccessible platform to explore a new parameter space for Kerr frequency comb generation. Two-cycle cavity soliton can be achievable with a high repetition rate, which opens great opportunities in integrated nonlinear photonics. Compared to optical solitons in a straight waveguide, the cavity soliton is more robust to dispersive and nonlinear perturbations. It is important to mention that the considered cavity Q-factor is not very high and can be obtained based on other materials platforms with much stronger nonlinearity such as silicon and chalcogenides, in which the nonlinear coefficient could be increased to be 100 times larger than what is used in this paper. This reveals a possibility to reduce the required pump power to the mW level, deliverable by integrated electrically pumped lasers. We expect that fully integrated on-chip comb generation will be achieved in the near future.

REFERENCES

[1] T. Udem, R. Holzwarth, T. W. Hänsch, "Optical frequency metrology," Nature 416, 233 (2002).

[2] S. T. Cundiff, J. Ye, "Colloquium: Femtosecond optical frequency combs," Rev. Mod. Phys. 75, 325 (2003).

[3] U. Keller, "Recent developments in compact ultrafast lasers," Nature 424, 831 (2003).

[4] C. Gohle, T. Udem, M. Herrmann, J. Rauschenberger, R. Holzwarth, H. A. Schuessler, F. Krausz, and T. W. Hänsch, "A frequency comb in the extreme ultraviolet," Nature 436, 234 (2005).

[5] I. Coddington, W. C. Swann, L. Nenadovic, and N. R. Newbury, "Rapid and precise absolute distance measurements at long range," Nat. Photonics 3, 351 (2009).

[6] C. B. Huang, Z. Jiang, D. Leaird, J. Caraquitena, and A. Weiner, "Spectral line-by-line shaping for optical and microwave arbitrary waveform generations," Laser Photonics Rev. 2, 227 (2008).

[7] T. Steinmetz, T. Wilken, C. Araujo-Hauck, R. Holzwarth, T. W. Hänsch, L. Pasquini, A. Manescau, S. D'Odorico, M. T. Murphy, T. Kentischer, W. Schmidt and T. Udem, "Laser frequency combs for astronomical observations," Science 321, 1335 (2008).

[8] N. R. Newbury, "Searching for applications with a fine-tooth comb," Nature Photonics 5, 186 (2011).

[9] D. K. Armani, T. J. Kippenberg, S. M. Spillane, K. J. Vahala, "Ultra-high-Q toroid microcavity on a chip," Nature 421, 925 (2003).

[10] T. J. Kippenberg, R. Holzwarth, and S. A. Diddams, "Microresonator-based optical frequency combs," Science 332(6029), 555–559 (2011).

[11] P. Del'Haye, A. Schliesser, O. Arcizet, T. Wilken, R. Holzwarth and T. J. Kippenberg, "Optical frequency comb generation from a monolithic microresonator," Nature 450, 1214 (2007).

[12] A. A. Savchenkov, A. B. Matsko, V. S. Ilchenko, I. Solomatine, D. Seidel, and L. Maleki, "Tunable optical frequency comb with a crystalline whispering gallery mode resonator," Physical Review Letters 101, 093902 (2008).

[13] I. S. Grudinin, N. Yu and L. Maleki, "Generation of optical frequency combs with a CaF2 resonator," Opt. Lett. vol. 34, 878-880 (2009).

[14] J. S. Levy, A. Gondarenko, M. A. Foster, A. C. Turner-Foster, A. L. Gaeta and M. Lipson, "CMOS-compatible multiple-wavelength oscillator for on-chip optical interconnects," Nature Photonics 4, 37-40 (2010).

[15] L. Razzari, D. Duchesne, M. Ferrera, R. Morandotti, S. Chu, B. E. Little, and D. J. Moss, "CMOS-compatible integrated optical hyper-parametric oscillator," Nat. Photon 4, 41 (2010).

[16] S. B. Papp and S. A. Diddams, "Spectral and temporal characterization of a fused-quartz-microresonator optical frequency comb," Phys. Rev. A 84, 053833 (2011).

[17] F. Ferdous, H. Miao, D. E. Leaird, K. Srinivasan, J. Wang, L. Chen, L. T. Varghese, and A. M. Weiner, "Spectral line-by-line pulse shaping of on-chip microresonator frequency combs," Nat. Photonics 5, 770-776 (2011).

[18] A. B. Matsko, A. A. Savchenkov, W. Liang, V. S. Ilchenko, D. Seidel, and L. Maleki, "Mode-locked Kerr frequency combs," Opt. Lett. 36, 2845-2847 (2011).

[19] T. Herr, V. Brasch, J. D. Jost,   C. Y. Wang, N. M. Kondratiev, M. L. Gorodetsky & T. J. Kippenberg," Temporal solitons in optical microresonators,"   http://arxiv.org/abs/1211.0733

[20] K. Saha, Y. Okawachi, B. Shim, J. S. Levy, R. Salem, A. R. Johnson, M. A. Foster, M. R. Lamont, M. Lipson, and A. L. Gaeta, "Modelocking and femtosecond pulse generation in chip-based frequency combs," Opt. Express 21, 1335-1343 (2013).

[21] F. Leo, S. Coen, P. Kockaert, S.-P. Gorza, P. Emplit, and M. Haelterman, "Temporal cavity solitons in one-dimensional Kerr media as bits in an all-optical buffer," Nature Photonics 4, 471-476 (2010).

[22] P. Del'Haye, T. Herr, E. Gavartin, M. L. Gorodetsky, R. Holzwarth, and T. J. Kippenberg, "Octave spanning tunable frequency comb from a microresonator," Phys. Rev. Lett. 107, 063901 (2011).

[23] Y. Okawachi, K. Saha, J. S. Levy, Y. H. Wen, M. Lipson, and A. L. Gaeta, "Octave-spanning frequency comb generation in a silicon nitride chip," Opt. Lett. 36, 3398 (2011).

[24] S. Coen and M. Erkintalo, "Universal scaling laws of Kerr frequency combs," Opt. Lett. 38, 1790 (2013).

[25] L. Yin, Q. Lin, and G. P. Agrawal, "Dispersion tailoring and soliton propagation in silicon waveguides," Opt. Lett. 31, 1295-1297 (2006).

[26] A. C. Turner, C. Manolatou, B. S. Schmidt, M. Lipson, M. A. Foster, J. E. Sharping, and A. L. Gaeta, "Tailored anomalous group-velocity dispersion in silicon channel waveguides," Opt. Express 14, 4357-4362 (2006).

[27] L. Zhang, Y. Yue, Y. Xiao-Li, R. G. Beausoleil and A. E. Willner, "Highly dispersive slot waveguides," Optics Express 17, 7095-7101 (2009).

[28] L. Zhang, Y. Yue, R. G. Beausoleil, and A. E. Willner, "Flattened dispersion in silicon slot waveguides," Opt. Express 18(19), 20529-20534 (2010).

[29] L. Zhang, Q. Lin, Y. Yue, Y. Yan, R. G. Beausoleil, and A. E. Willner, "Silicon waveguide with four zero-dispersion wavelengths and its application in on-chip octave-spanning supercontinuum generation," Optics Express 20, 1685-1690 (2012).

[30] Peter W. Nolte, Christian Bohley, and Jörg Schilling, "Tuning of zero group velocity dispersion in infiltrated vertical silicon slot waveguides," Opt. Express 21, 1741-1750 (2013)

[31] L. Zhang, Y. Yan, Y. Yue, Q. Lin, O. Painter, R. G. Beausoleil, and A. E. Willner, "On-chip two-octave supercontinuum generation by enhancing self-steepening of optical pulses," Optics Express 19, 11584–11590 (2011).

[32] L. Zhang, A. M. Agarwal, L. C. Kimerling, and J. Michel, "Nonlinear group IV photonics based on silicon and germanium: from near-infrared to mid-infrared," Nanophotonics, 2014.

[33] S. Wang, J. Hu, H. Guo, and X. Zeng, "Optical Cherenkov radiation in an As2S3 slot waveguide with four zero-dispersion wavelengths," Optics Express 21, 3067 (2013)

[34] Z. Jafari and F. Emami, "Strip/slot hybrid arsenic tri-sulfide waveguide with ultra-flat and low dispersion profile over an ultra-wide bandwidth," Optics Letters 38, 3082-3085 (2013)

[35] S. Afshar V. and T. M. Monro, "A full vectorial model for pulse propagation in emerging waveguides with subwavelength structures part I: Kerr nonlinearity," Opt. Express 17, 2298-2318 (2009)

[36] A. Gondarenko, J. S. Levy, and M. Lipson, "High confinement micron-scale silicon nitride high Q ring resonator," Opt. Express 17, 11366-11370 (2009)

[37] K. K. Lee, D. R. Lim, L. C. Kimerling, J. Shin, and F. Cerrina, "Fabrication of ultralow-loss Si/SiO2 waveguides by roughness reduction," Opt. Lett. 26, 1888-1890 (2001)

[38] M. Haelterman, S. Trillo, and S. Wabnitz, "Dissipative modulation instability in a nonlinear dispersive ring cavity," Opt. Commun. 91, 401-407 (1992).

[39] L. A. Lugiato and R. Lefever, "Spatial dissipative structures in passive optical-systems," Physical Review Letters 58, 2209 (1987).

[40] S. Coen, H. G. Randle, T. Sylvestre, and M. Erkintalo, "Modeling of octave-spanning Kerr frequency combs using a generalized mean-field Lugiato-Lefever model," Opt. Lett. 38, 37-39 (2013).

[41] Y. K. Chembo and C. R. Menyuk, "Spatiotemporal Lugiato-Lefever formalism for Kerr-comb generation in whispering-gallery-mode resonators," Physical Review A 87, 053852 (2013).

[42] Q. Lin, O. J. Painter, and G. P. Agrawal, "Nonlinear optical phenomena in silicon waveguides: modeling and applications," Opt. Express 15, 16604-16644 (2007)

[43] J. M. Dudley, G. Genty, and S. Coen, "Supercontinuum generation in photonic crystal fiber," Rev. Mod. Phys. 78, 1135–1184 (2006).

[44] M. R. E. Lamont, Y. Okawachi, and A. L. Gaeta, "Route to stabilized ultrabroadband microresonator-based frequency combs," Opt. Lett. 38, 3478-3481 (2013)

[45] G. P. Agrawal, [Nonlinear Fiber Optics], 4th ed., Academic Press (San Diego, California, 2007).